Magnetic First-Order Phase Transition in Single-Crystal MnAs

R. W. De Blois* and D. S. Rodbell
General Electric Research Laboratory, Schenectady, New York
(Received 8 January 1963)

This paper describes an experimental and theoretical examination of a 10-μg c-axis-oriented single crystal of MnAs. The critical magnetic field for the first-order transition to the ferromagnetic phase has been measured as a function of temperature (15 to 65°C) and pressure (0 to 1000 bars gauge), using miniature-coil pulsed fields to 110 kOe. Data analysis substantiates the thesis of the recent Bean-Rodbell theory on magnetic first-order phase transitions that the transition in MnAs near 45°C is between ferromagnetic and paramagnetic phases and arises from a sufficiently sensitive dependence of exchange energy on lattice strain and a sufficiently high compressibility. The match between theory and experiment yields a compressibility K of 4.55×10^{-12} dyn^{-1} cm^2, a lattice thermal expansion coefficient α of 5.71×10^{-5}/°C, an apparent paramagnetic Curie temperature T_0^* of 277.1°K, and a Curie-temperature dependence on volume strain, β $[\equiv(dT_c/T_0)(dV/V_0)^{-1}]$, of 18.9, where T_0 is the Curie temperature of the unstrained specimen at 0°K. Discrepancies in the match suggest a primary need to include short-range order in the theory. Auxiliary experiments show the magnetocrystalline anisotropy sum, $K_1+2K_2+3K_3$, to be about -7.6 and -12.0×10^6 ergs/cm^3 at 299 and 77°K, respectively.

INTRODUCTION

MANGANESE arsenide has long been known to be ferromagnetic[1] and to undergo an abrupt loss of ferromagnetism near[2] 45°C with a large accompanying density increase,[3] which x-ray measurements show to be 1.86%,[4] and a latent heat of 1.79 cal/g.[5] A temperature hysteresis of about 10°C for the return to ferromagnetism is also observed.[6,7]

The nature of this transition has, until recently, been unclear. Susceptibility measurements by Bates[7] and by Serres[8] show an anomalous region between 45 and 126°C. Only above 126°C does the material follow the Curie-Weiss law. Guillaud[9] obtained magnetization data below 45°C in fields to 20 000 Oe and found that a plot of the square of the saturation magnetization versus temperature extrapolated to a virtual Curie temperature of 130°C. This result and Serres's data suggested to him and Meyer[10] that the transition at 45°C was from ferromagnetism to antiferromagnetism, and at 126°C from antiferromagnetism to paramagnetism. However, Kurti noted in the discussion following Guillaud's paper that the entropy change at 45°C was larger than one would expect for a transition between two ordered magnetic phases. Strongly supporting Guillaud and Meyer's interpretation were Meyer and Taglang's observations of specific-heat[10] and magnetocaloric-effect[11] anomalies near 126°C. More recently, Kittel[12] has developed a theory involving "exchange inversion" to explain the antiferromagnetic to ferromagnetic transition of Cr-doped Mn_2Sb, and extends the treatment to include a ferromagnetic to antiferromagnetic transition in MnAs. He recognizes, however, that this development might not apply specifically to MnAs.

On the other hand, Bacon and Street[13] found no evidence from neutron diffraction data that the postulated antiferromagnetic phase exists. Furthermore, Rodbell[14] concluded from electron-spin resonance data he took at various temperatures that either the transition near 45°C is to the paramagnetic, not the antiferromagnetic, phase or that the antiferromagnetic phase, if it exists, has a very small exchange field.

In view of these discrepancies, Bean and Rodbell[15] chose to examine theoretically the possibility of a first-order transition from the ferromagnetic to paramagnetic phases. They find that such a transition will occur if the exchange interaction varies sufficiently with lattice dimensions and if the lattice is sufficiently compressible with respect to the pertinent dimensions. They show that the known experimental data on MnAs are in substantial agreement with the theory and derive values for the compressibility and for the strain sensitivity of the exchange interaction that appear reasonable, though neither quantity has as yet been directly measured. In addition, the generalized theory encompasses other first- and second-order transitions for materials with

* This work is based on a thesis submitted to the Department of Physics of Rensselaer Polytechnic Institute, Troy, New York, by R. W. DeBlois in partial fulfillment of the requirements for the Ph.D. degree.

[1] F. Heusler, Z. Angew. Chem. **17**, 260 (1904).
[2] S. Hilpert and T. Dieckmann, Ber. Deut. Chem. Ges. **44**, 2378 and 2831 (1911). Also, S. Hilpert, T. Dieckmann, and E. Colver-Glauert, Trans. Faraday Soc. **8**, 207 (1912).
[3] A. Smits, H. Gerding, and F. Ver Mast, Z. Physik. Chem. Bodenstein Festband (Leipzig), 357 (1931).
[4] B. T. M. Willis and H. P. Rooksby, Proc. Phys. Soc. (London), **B67**, 290 (1954).
[5] L. F. Bates, Proc. Roy. Soc. (London), **A117**, 680 (1928).
[6] Footnote in S. Hilpert and J. Beyer, Ber. Deut. Chem. Ges. **44**, 1608 (1911).
[7] L. F. Bates, Phil. Mag. **8**, 714 (1929).
[8] A. Serres, J. Phys. Radium **8**, 146 (1947).
[9] C. Guillaud, J. Phys. Radium **12**, 233 (1951); also thesis, University of Strasbourg, 1943 (unpublished).
[10] A. J. P. Meyer and P. Taglang, J. Phys. Radium **12**, 63S (1951).
[11] A. J. P. Meyer and P. Taglang, Compt. Rend. **246**, 1820 (1958).
[12] C. Kittel, Phys. Rev. **120**, 335 (1960).
[13] G. E. Bacon and R. Street, Nature **175**, 518 (1955).
[14] (Unpublished), but see W. B. Pearson, in *Handbook of Lattice Spacings and Structures of Metals and Alloys* (Pergamon Press, Inc., New York, 1958), p. 58.
[15] C. P. Bean and D. S. Rodbell, Phys. Rev. **126**, 104 (1962); J. Phys. Soc. Japan **17**, Suppl. B-I, 154 (1962).

various values of the above quantities and of the lattice thermal expansion coefficient.[16]

During the developmental period of the Bean-Rodbell theory, their colleagues, Kasper and Wilson,[17] obtained neutron diffraction data of increased precision on MnAs and concluded that less than a few percent of full order exists for any simple model of the antiferromagnetic phase. In addition, they have obtained detailed x-ray data on a single crystal that confirm the existence of the hexagonal NiAs-type structure in the ferromagnetic phase and above 125°C, but that show a slight orthorhombic distortion in the anomalous region in between.[18] Kornelsen[19] has also found this distortion by using powder x-ray methods of high resolution and observes that it disappears at 125°C. These neutron and x-ray data results suggested to Bean and Rodbell[15] that a Jahn-Teller distortion exists in the intermediate region and that the specific heat, magnetocaloric, and susceptibility anomalies near 125°C are associated with the loss of this distortion and not with the disappearance of a cooperative magnetic phase.

Also during this period experimental developments leading to the use of miniature pulsed-field coils[20] made it possible to obtain detailed magnetic-transition data on a 10 μg, c-axis-oriented, single crystal of MnAs in pulsed fields to 110 kOe, at pressures to 1000 bars, and in the temperature range from 15 to 65°C.[21] In this paper we analyze these data in terms of the Bean-Rodbell theory. We find surprisingly close agreement in view of the approximations made and the recognized shortcomings of the theory in its present form. The analysis, furthermore, provides a systematic means for deriving values for the compressibility, strain sensitivity of the exchange interaction, apparent paramagnetic Curie temperature, and lattice thermal expansion coefficient. Lastly, there now remains little doubt that the transition in MnAs near 45°C is between ferromagnetic and paramagnetic phases.

THEORY

The usual transition from an ordered to a disordered magnetic phase, occurring as the system passes through the Curie temperature, is of second order and is associated with discontinuous changes in the specific heat, magnetocaloric effect, susceptibility, volume magnetostriction, compressibility, and thermal expansion coefficient. These quantities involve second-order derivatives of the Gibbs free-energy function modified to include magnetization energy. A reversible first-order magnetic phase transition, on the other hand, is said to occur when there are discontinuous changes in entropy, volume, and saturation magnetization, and thus in the first-order derivatives of the Gibbs free energy, while the temperature, pressure, and applied magnetic field remain constant.

Bean and Rodbell[15] show that the transition between phases of magnetic order and disorder, for example, from the ferromagnetic to the paramagnetic phases in MnAs, will be of first order if the exchange interaction is a sufficiently strong function of some lattice parameter and if that parameter has a sufficiently large strain to stress modulus. To simplify the theory, they choose the lattice volume as the parameter and the isothermal compressibility as the modulus. It is recognized that this cannot be an accurate representation for MnAs since the transition at 45°C involves anisotropic strains, with the distance between nearest-neighbor manganese ions remaining almost constant.

The model they consider is of a collection of interacting magnetic dipoles with the interaction taken as that of the molecular-field approximation. The central assumption of the model is given in Eq. (1).

$$T_c = T_0[1+\beta(V-V_0)/V_0], \tag{1}$$

where T_c is the Curie temperature (a measure of the exchange energy), and T_0 is the Curie temperature that the system would have if the specific volume V were restrained to equal V_0, the specific volume at 0°K in the absence of strains introduced by exchange interactions or externally applied stresses. β, assumed to be constant in the neighborhood of V_0, is the dimensionless slope, $d(T_c/T_0)/d(V/V_0)$, of the dependence of T_c on volume.

The Gibbs free energy per unit mass of a magnetic system is defined as

$$G = U - TS - H\sigma_0\sigma + PV, \tag{2}$$

where U is the internal energy per unit mass, σ_0 is the saturation magnetic moment per unit mass at 0°K, and σ is the relative magnetization. Then, within the molecular-field approximation and for arbitrary spin j, the theory assumes the Gibbs free energy per gram of magnetic material to be

$$G = -\frac{3}{2}\frac{j}{j+1}NkT_c\sigma^2 + \frac{1}{2K}\frac{(V-V_0)^2}{V_0} - T[S_j+S_l] - H\sigma_0\sigma + PV, \tag{3}$$

where N is the number of magnetic ions per gram; k is the Boltzmann constant; $K[\equiv -V^{-1}(\partial V/\partial P)_{T,H}]$ is the isothermal compressibility, assumed to be constant; T is the absolute temperature; S_j and S_l are the entropies per gram of the spin system and lattice, respectively; H is the applied magnetic field; and P is the pressure.

[16] D. S. Rodbell and C. P. Bean, J. Appl. Phys. **33**, 1037 (1962). D. S. Rodbell, Phys. Rev. Letters **7**, 1 (1961).

[17] J. S. Kasper and R. H. Wilson (private communication).

[18] R. H. Wilson and J. S. Kasper, American Crystallographic Association 1961 Annual Meeting, Abstract M-8.

[19] R. O. Kornelsen, Can. J. Phys. **39**, 1728 (1961).

[20] R. W. DeBlois, Rev. Sci. Instr. **32**, 816 (1961).

[21] R. W. DeBlois, in *Proceedings of International Conference on High Magnetic Fields, Massachusetts Institute of Technology, Cambridge, Massachusetts, 1961*, edited by H. Kolm, B. Lax, F. Bitter, and R. Mills (Technology Press, Cambridge, Massachusetts, 1962) p. 568. [Accidently missing from the text are phrases mentioning the use of a two-turn pickup coil (p. 568) and the abruptness for the single-crystal specimen of the PM to FM transition (p. 570).]

The equation of state of a magnetic system will involve three independent variables, for example, H, T, and P. For materials such as MnAs the equations of state are only rudimentally known. However, if H, T, and P are fixed, we may note that the dependent variables σ, S_j, S_l, and V will ideally assume such values as will minimize the free energy. As a first step in determining what the minimizing values of σ and V are, we may assume σ, and thus also S_j in the molecular-field approximation, to be fixed and will then find the value of V which minimizes the free energy. To do this we substitute Eq. (1) in Eq. (3), take the partial derviative of the resulting equation with respect to V, holding H, T, P, and σ constant, set $\partial G/\partial V$ equal to zero, and solve for V. We obtain

$$\frac{V-V_0}{V_0}=-\frac{3}{2}\frac{j}{j+1}\frac{NkKT_0\beta\sigma^2}{V_0}+\alpha T-PK. \tag{4}$$

The αT term, in which α $[\equiv V^{-1}(\partial V/\partial T)_{P,H}]$ is the lattice thermal expansion coefficient, results from the approximate expression $\partial S_l/\partial V \doteq \alpha/K$, which derives from the expression

$$S_l \doteq C_v \ln T+\alpha(V-V_0)/K, \tag{5}$$

which in turn is derived[15] under the assumption of constant α and C_v, the specific heat at constant volume.

Thus, the Gibbs free energy that is a minimum with respect to V, though not yet with respect to σ, is, from Eqs. (1), (3), (4), and (5),

$$G=-\frac{9}{8}\left(\frac{j}{j+1}\right)^2(NkT_0\beta)^2\frac{K\sigma^4}{V_0}$$
$$-\frac{3}{2}\frac{j}{j+1}NkT_0[1-\beta(PK-\alpha T)]\sigma^2-H\sigma_0\sigma$$
$$-TS_j-TC_v\ln T-\frac{\alpha^2T^2V_0}{2K}+PV_0(1+\alpha T-\tfrac{1}{2}PK). \tag{6}$$

The next step in determining the minimum Gibbs free energy for given values of H, T, and P is to calculate and plot $[G(\sigma)-G(0)]$ versus σ from Eq. (6) for various values of H, T, and P. The lowest minimum in such a curve will give the relative magnetization σ and thus also the specific volume V that correspond to the thermodynamic equation of state of the system for the given values of H, T, and P. In addition, however, such curves permit us to examine the nonequilibrium metastable states of the system. The necessary conditions for the existence of such metastable states, leading to first-order transitions, are described in the Bean-Rodbell papers.[15,16] Briefly, the spin entropy in the molecular field approximation is a function $S_j(\sigma)$ of the relative magnetization σ. The authors develop $S_j(\sigma)$ as a series in even powers of σ and then express the minimized free energy of Eq. (6) in a power series in σ. In comparing terms of the fourth power in σ, they find it convenient

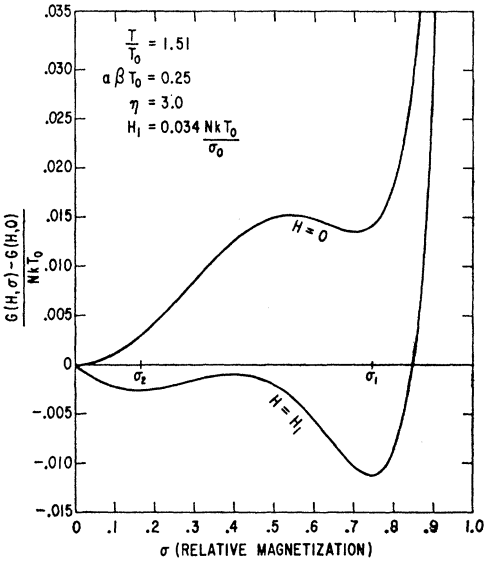

FIG. 1. Net Gibbs free energy/NkT_0 vs relative magnetization σ for applied magnetic fields zero and H_1. For a system initially at $\sigma=0$ with $H=0$, applying the field H_1 depresses the system's free energy to the metastable state at σ_2 or, with barrier penetration, to the stable state at σ_1.

to make the substitution

$$\eta_j\equiv-\frac{5}{2}\frac{[4j(j+1)]^2}{[(2j+1)^4-1]}\frac{NkKT_0\beta^2}{V_0}. \tag{7}$$

Then they show that the condition at zero field for the possible existence of a potential barrier and thus of a first-order phase transition is

$$\eta_j>1-\beta(PK-\alpha T). \tag{8}$$

As an illustration of the significance of this additional feature we may note in Fig. 1 of net Gibbs free energy/NkT_0 versus relative magnetization σ that the equilibrium value of σ is σ_1 for applied magnetic field H_1. However, a fast magnetic-field pulse acting for only a few microseconds on a system initially in equilibrium with $\sigma=0$ at $H=0$ may merely raise σ to the metastable state at σ_2 during this instant, instead of to σ_1. Thus experiments taking place in a time short compared to the time required, through the formation or growth of nuclei, to penetrate the potential barriers involved will yield nonequilibrium states.

To explore further the system's behavior in a pulsed field we may qualitatively examine Fig. 2. Curve A is a plot of net free energy $[G(\sigma)-G(0)]$ versus σ for zero field and fixed values of temperature and pressure. (We ignore the constant factor $NkT_0\times10^{-3}$ temporarily.) It is apparent from the graph and from Eq. (6) that subtracting a term linear in σ and having a slope of free energy versus σ parallel to the double tangent line shown will produce curve B, and that this curve corresponds to that applied magnetic field, H_1, for the given temperature and pressure, for which the paramagnetic and

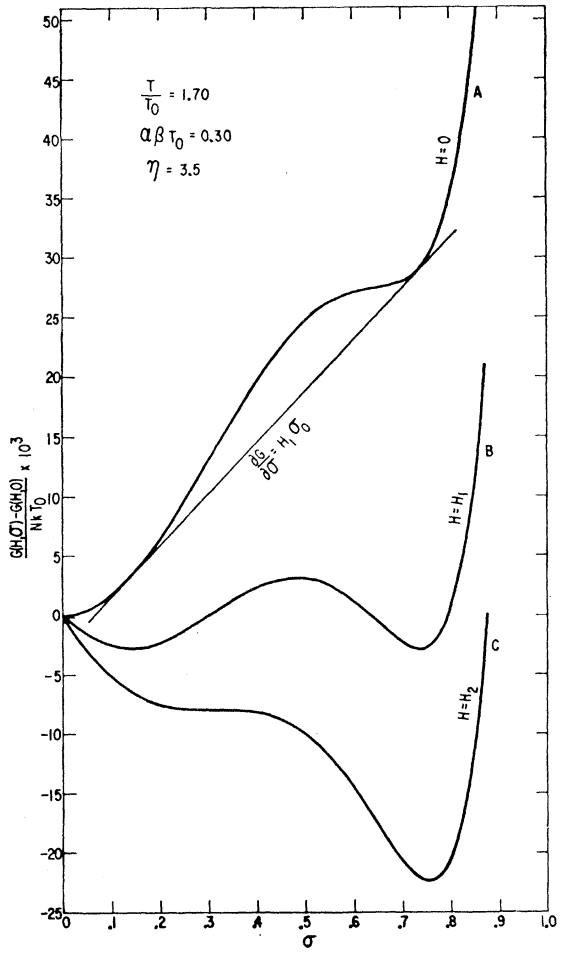

FIG. 2. Free energy vs relative magnetization σ for three magnetic-field values. Application of field H_1 or H_2 depresses the zero-field curve A to equilibrium curve B or to "zero-barrier" curve C, respectively. Field H_2 is proportional to the slope of curve A at inflection point $\sigma=0.32$.

ferromagnetic phases are in thermodynamic equilibrium. Subtraction of a certain larger field term, $H_2\sigma_0\sigma$, corresponding to the slope of curve A at the inflection point at $\sigma=0.32$, yields the "zero-barrier" curve C. (The corresponding "zero-barrier" curve for the ferromagnetic to paramagnetic transition would lie just below curve A and would result from subtraction of the term $H_3\sigma_0\sigma$ from curve A, where $H_3\sigma_0$ is the slope of curve A at the inflection point at $\sigma=0.65$.) Therefore, at a given temperature and pressure the experimentally observed magnetic field that produces the paramagnetic to ferromagnetic transition should lie somewhere between the values H_1 and H_2. For fast pulsed fields giving little time for nucleation of the ferromagnetic phase it might be close to H_2, while for dc measurements it will be nearer to H_1. (The specific nature of the imperfection permitting the formation of a nucleus and how this formation depends on time is presently unclear.) Moreover, the field difference, H_2-H_3, corresponding to the two "zero-barrier" curves, represents the maximum possible isothermal hysteresis. In a pulsed field, however, semiadiabatic processes prevail. The transition to the ferromagnetic phase orders the spin system, which must then contribute entropy to the lattice and thus raise the specimen's temperature. This reduces the theoretical and actual hysteresis fields for the beginning of the return to the paramagnetic phase.

Since curve C of Fig. 2 has an inflection point at $\sigma=0.32$, one may also find the conditions for such a "zero-barrier" curve by taking the first and second partial derivatives of Eq. (6) with respect to σ and setting each derivative equal to zero. This procedure yields

$$\frac{H\sigma_0}{NkT_0}=-\frac{T}{T_0}\left[\frac{1}{Nk}\frac{\partial S_j}{\partial\sigma}+\frac{3j}{j+1}\alpha\beta T_0\sigma\right]$$
$$-\frac{3j}{j+1}[1-PK\beta]\sigma-\frac{9}{80}\frac{[(2j+1)^4-1]}{(j+1)^4}\eta_j\sigma^3, \quad (9)$$

and

$$\frac{T}{T_0}=\left(\frac{3j}{j+1}[1-PK\beta]+\frac{27}{80}\frac{[(2j+1)^4-1]}{(j+1)^4}\eta_j\sigma^2\right)\Big/$$
$$\left(-\frac{1}{Nk}\frac{\partial^2 S_j}{\partial\sigma^2}-\frac{3j}{j+1}\alpha\beta T_0\right). \quad (10)$$

Then if $\partial^2 S_j/\partial\sigma^2$ and $\partial S_j/\partial_0$ are known for a given $\sigma(<0.5)$, and the parameters are assigned known or assumed values, one may first determine T/T_0 from Eq. (10). Substituting this T/T_0 into Eq. (9) yields the magnetic field H required to produce the "zero-barrier" condition for the paramagnetic to ferromagnetic transition at the given σ.

EXPERIMENT

The experimental arrangement of the MnAs specimen and pickup coil with respect to the miniature field coil is shown to scale in Figs. 3. The single-crystal specimen, glued inside the two-turn pickup coil with polystyrene dope, is a powder grain 296 μ long, 90 μ wide, and 25 μ thick, picked from a thermally fractured sample prepared from 14.35 g of 99.84% Foote Mineral Co.

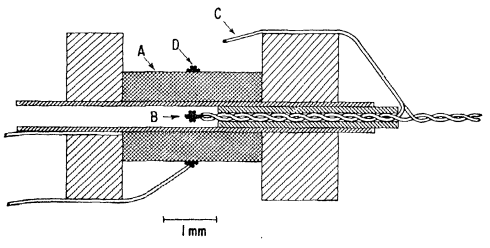

FIG. 3. Diagram of miniature pulsed-field coil, A, 2.62-mm long, containing a 10-μg MnAs specimen, B, inside a two-turn pickup coil, one strand of which is looped in a critical position, C, outside the field coil to cancel the dH/dt signal. Six counter turns, D, about the field coil flatten the central axial field contour.

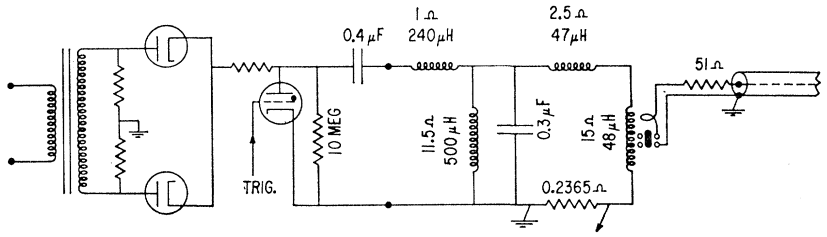

FIG. 4. Schematic high-field pulse-circuit diagram. The 0.4 μF condenser, storing up to 5 J of energy, discharges into a pulse-shaping network containing the 48 μH field coil.

manganese and 15.00 g of 99.999% American Smelting and Refining Co. arsenic. The mixed powders were contained in an alumina tube which was sealed inside a quartz tube evacuated to 5×10^{-5} mm of Hg, heated at 1000°C for 14 h, and slowly cooled. Chemical analysis of the sample yields a composition of 49.9 at.% Mn and 50.1 at.% As.

X-ray analysis shows the long axis of the specimen to be the c axis. Since the lattice discontinuity in MnAs as it passes through its first-order transition is almost wholly in the basal plane, elongated fragments with such orientation are to be expected.[22] The loose specimen lines up perpendicular to the field ($\sim$100 Oe) of an Alnico magnet, thus indicating that the c axis of the hexagonal lattice is the hard direction of magnetization and that the magnetocrystalline anisotropy is large. That the magnetic moments lie in or near the basal plane also appears probable from the recent neutron diffraction data of Kasper and Wilson[17] and from the earlier ones of Bacon and Street.[13]

One strand of the twisted pickup-coil leads, which pass through and are glued to the inner quartz capillary, is led over and glued to one plastic end plate to form a loop near the field coil. With critical adjustment of its position it is possible to cancel almost completely the signal proportional to dH/dt, leaving only the signal proportional to $d\sigma/dt$ resulting from the abrupt change in magnetization at the transition.

The field coil, 2.62 mm long and 1.70 mm in outside diameter, is wound on a 595 μ o.d. quartz capillary. It contains 441 turns of 50 μ copper wire insulated with Formex to a diameter of 61 μ. The lead of the first of the ten layers enters through an inner groove in one end plate. The lead from the tenth layer is glued to the rim of this same end plate, is then led to the outside center of the coil to form six counter turns, and is then passed back over the end plate. Pulse tests at constant temperature with the specimen used as a probe indicate that the field in the central 400 μ of the coil is flat to about $\frac{1}{2}$%. Calculation indicates that adding several more counter turns would produce an even flatter field contour. The calculated net field at the coil center is 1800 Oe/Å.[23]

The pulse circuit is shown schematically in Fig. 4. The thyratron-triggered pulser charges a 0.4-μF condenser to a maximum of 5 kV and thus stores a maximum of 5.0 J. The values of the components in the external pulse-shaping network were varied experimentally to arrive at a suitable shape and duration for the field pulse. Calculation shows that a 100-kOe, 25-μsec pulse would heat the wire of the 48 μH, 15 Ω (at room temperature) field coil about 40°C under adiabatic conditions. Experimentally, this results in only a several degree rise in the specimen temperature after the pulse is over. To start from thermal equilibrium, data were taken at intervals of not less than three minutes after the prior pulse.

The field coil and specimen are enclosed inside an oil-filled hydraulic pressure cell connected to a Carver Laboratory press. Six Teflon-insulated "golf tees" serve as electrical leads through the cell for the pulse, pickup coil, and thermocouple leads.[24] The pickup-coil leads and the voltage leads over the 0.2365 Ω standard pulse-probe resistance (nominally 0.227 Ω) go to type L and K plug-in units, respectively, in a dual beam Tektronix 551 oscilloscope, from which Polaroid prints of the traces are obtained. The field-trace voltages are calibrated against photographs of the oscilloscope's square-wave calibration voltage, which is checked on occasion with a dc voltmeter at the internal calibration test-point. A Tektronix 535 oscilloscope is used for visual monitoring and for applying a delayed trigger to the 551. The 125 μ diameter Chromel P-Alumel thermocouple leads inside the cell end within 1 mm of the field-coil surface. Their leads through the cell are machined from Chromel P and Alumel rods. A Rubicon model 2732 potentiometer with an ice junction is used for measuring the temperature. Glass heating tape wrapped around the outside of the pressure cell is used to maintain temperatures above room temperature. Styrofoam and paper serve for thermal insulation. Marsh Instrument Co. and Fred S. Carver pressure gauges, with ranges 0–2000 psi and 0–16 000 psi, respectively, both calibrated against standards at the General Electric Advanced Technology Laboratory, serve for pressure measurements.

EXPERIMENTAL RESULTS

The lower oscilloscope traces in Fig. 5(a) show the voltage over the 0.2365 Ω standard resistance versus time during a 25-μsec pulse and indicate a peak field of

[22] Z. S. Basinski and W. B. Pearson, Can. J. Phys. **36**, 1017 (1958).

[23] See, for example, R. M. Bozorth, *Ferromagnetism* (D. Van Nostrand Company, Inc., New York, 1951), p. 840.

[24] For a review of current high-pressure techniques for solid state physics see, e.g., C. A. Swenson, in *Solid State Physics*, edited by F. Seitz and D. Turnbull (Academic Press Inc., N. Y., 1960), Vol. 11, p. 41. The 1000-bar maximum pressure of the present experiment scarcely qualifies as a high pressure.

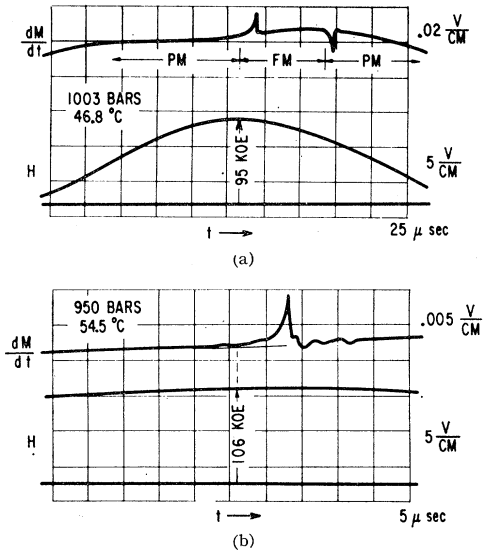

FIG. 5. (a) Oscilloscope traces of a field pulse rising to 95 kOe and of the accompanying net pickup-coil voltage indicating a paramagnetic to ferromagnetic transition at the field peak and the subsequent reverse transition at 74 kOe. (b) Expanded oscilloscope trace of a similar paramagnetic to ferromagnetic transition.

95 kOe. The upper trace of net pickup-coil voltage, proportional to the time rate of change of magnetization, indicates the occurrence of a paramangetic to ferromagnetic transition at this peak field, as well as the reverse transition, with 21-kOe hysteresis, at 74 kOe. Figure 5(b) shows a similar paramagnetic to ferromagnetic transition at higher amplification and sweep speed. The field amplitude is adjusted so that the paramagnetic to ferromagnetic transition occurs near the peak, since the field at which the transition appears to start increases by as much as 2% if the transition occurs as the field is still rapidly rising. (This effect may be due to semiadiabatic heating of the specimen.) The field data are taken at the beginning of the transition, since it is observed that a transition starting at or even apparently slightly beyond the field peak will continue to completion. Occasionally a transition that appears to start as the field is decreasing will not go to completion. In such cases the hysteresis is reduced by about one-quarter.

A small region of detailed data for the paramagnetic to ferromagnetic transition as a function of temperature, pressure, and magnetic field is shown in Fig. 6. The numbers to one side of the diagonal line indicate the height above the $H=0$ plane of the surface separating the paramagnetic and ferromagnetic phases for the paramagnetic to ferromagnetic transition. The diagonal line defines the sharp lower limits of temperature and pressure at zero field at which the single-crystal specimen still remains paramagnetic, in a critical metastable state, for time durations of at least several minutes. The crosses indicate data points at which the specimen was found to be initially ferromagnetic, i.e., no transition occurred on applying an adequately high pulsed field

TABLE I. Transition-field data from Fig. 7.

H (kOe)	0 bars T (°C)	1000 bars T (°C)	H (kOe)	0 bars T (°C)	1000 bars T (°C)
29	33.8		75	(66.0)	36.0
35	37.2	16.3	80		38.7
40	40.0	17.9	90		44.7
50	45.7	22.2	100		50.4
60	51.4	27.5	110		56.0
70	60.2	33.3			

to the specimen. We note, however, that if the specimen is known to be paramagnetic but is close to the transition line, application of a pulsed field as small as one-third the critical field will bring about the transition. Since this transition is not observable with the pickup coil, it is presumably a slow one which may arise by nucleation from a hydraulic rarefaction wave resulting from the pulse.

The accumulated data, representing about 800 points for fields to 110 kOe, pressures to 1000 bars, and temperatures from 15 to 65°C, are displayed in Fig. 7. Equifield contours extending from 40 to 110 kOe define the surface at which the paramagnetic to ferromagnetic transition takes place in pulsed fields. The line extending from 29 to 35 kOe, an extension of the diagonal line of Fig. 6, may be viewed as a vertical cliff separating the paramagnetic and ferromagnetic phases for the paramagnetic to ferromagnetic transition. At the base of the cliff the specimen is ferromagnetic in zero field. The existence of the cliff appears to depend on conditions of metastability discussed with regard to Fig. 1. Corresponding field versus temperature ($P=0$) data by Meyer and Taglang,[25] taken in the field of an electromagnet to 30 kOe, form a straight line with a slope of 3.0 kOe/°C. (Guillaud's[9] earlier data give a

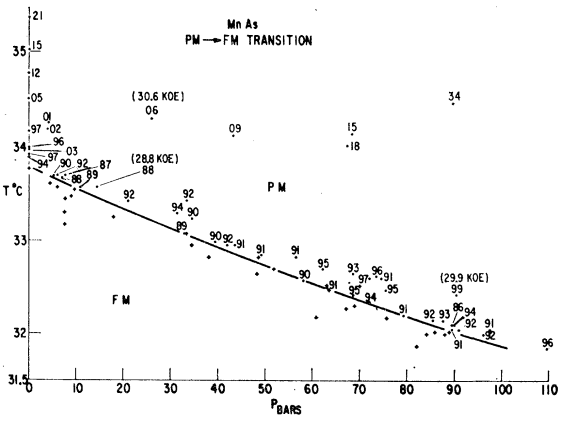

FIG. 6. H–P–T plot for the MnAs paramagnetic to ferromagnetic phase transition in pulsed magnetic fields. Below the diagonal line the specimen is ferromagnetic in zero field. Above this line it is paramagnetic up to the fields indicated by the numbers. (The fields range from 28.6 to 33.4 kOe. 86 represents 28.6 kOe, 34 represents 33.4 kOe, etc.)

[25] A. J. P. Meyer and P. Taglang, J. Phys. Radium **14**, 82 (1953).

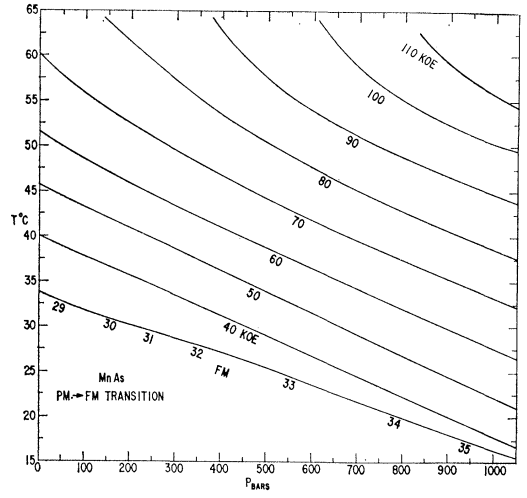

FIG. 7. *H–P–T* plot, of which Fig. 6 is a detailed section, for the MnAs paramagnetic to ferromagnetic phase transition in pulsed magnetic fields. The equi-field contours from 40 to 110 kOe and the "cliff" line extending from 29 to 35 kOe outline the surface above which the specimen is ferromagnetic. At the base of the "cliff" the specimen is ferromagnetic in zero field.

slope of about 1.5 kOe/°C.) They observe an isothermal hysteresis of about 30 kOe.

Table I shows field versus temperature data obtained from Fig. 7 at gauge pressures of zero and 1000 bars for the paramagnetic to ferromagnetic phase transition. These data will be used in the following analysis.

ANALYSIS

Paramagnetic susceptibility-temperature measurements above 126°C by Serres[8] yield an apparent Curie constant C* of 2.00×10^{-2}°C g^{-1} and an apparent Curie temperature T_0* of 285°K for a MnAs specimen provided by Guillaud. We note, however, that in accord with Eq. (1) the Curie temperature T_c changes with thermal expansion. Thus, we may write the Curie-Weiss law for the observed paramagnetic susceptibility, χ, as

$$\chi=\frac{C}{T-T_c}=\frac{C}{T-T_0(1+\alpha\beta T)}=\frac{C^*}{T-T_0^*}, \tag{11}$$

where

$$C^*\equiv\frac{C}{1-\alpha\beta T_0} \quad \text{and} \quad T_0^*\equiv\frac{T_0}{1-\alpha\beta T_0}.$$

A value for $\alpha\beta T_0$ of about 0.23 appears probable from the analysis to follow. Thus Serres's corrected Curie constant is about 1.54×10^{-2}°C g^{-1}. From theory[26]

$$C=N\mu_B^2g^2j(j+1)/3k, \tag{12}$$

where N is the number of magnetic ions per gram (4.64×10^{21} for MnAs), μ_B is the magnetic moment of the Bohr magneton, k is the Boltzmann constant, g is the gyromagnetic ratio (~2), and j is the spin quantum number, with possible values $\frac{1}{2}$, 1, $\frac{3}{2}$, etc. For a value of $j=\frac{3}{2}$, Eq. (12) gives a value for C of 1.45×10^{-2}°C g^{-1}. This is the same value for j that Guillaud[9] determined as probable.

After substitution of this value of $\frac{3}{2}$ for j in Eqs. (6) and (7) (and after droping the subscripts on $\eta_{3/2}$ and $S_{3/2}$ for convenience), we may obtain

$$\frac{G(\sigma)-G(0)}{NkT_0}=-0.1836\eta\sigma^4-0.9[1-\beta(PK-\alpha T)]\sigma^2 -\frac{H\sigma_0\sigma}{NkT_0}+\frac{T}{T_0}\left(\frac{S(0)-S(\sigma)}{Nk}\right). \tag{13}$$

Also, for $j=\frac{3}{2}$, Eqs. (9) and (10) become, respectively,

$$\frac{H\sigma_0}{NkT_0}=-0.7344\eta\sigma^3-1.8(1-PK\beta)\sigma -\frac{T}{T_0}\left(\frac{1}{Nk}\frac{\partial S}{\partial\sigma}+1.8\alpha\beta T_0\sigma\right), \tag{14}$$

and

$$\frac{T}{T_0}=\frac{2.2032\eta\sigma^2+1.8(1-PK\beta)}{-(1/Nk)(\partial^2S/\partial\sigma^2)-1.8\alpha\beta T_0}. \tag{15}$$

We may now proceed with the above three equations to search for the set of parameters, $\alpha\beta T_0$, η, and $K\beta$, that yields the best match with the experimental results listed in Table I. (From Eq. (1) we see that $\alpha\beta T_0$ is the slope of the curve showing Curie temperature T_c versus temperature T, and that $-K\beta$ is the slope of the curve showing T_c/T_0 versus pressure P, all for constant α, β, and K.) We note that tables of the entropy function of a collection of spins for values of j including $\frac{3}{2}$ have been calculated by Schmid and Smart.[27] The first and second derivatives with respect to σ may be calculated by numerical differentiation of the tables.

We shall assume a value for σ_0 of 130 emu/g. This is less than Guillaud's[9] value of 138 emu/g, and slightly greater than Rodbell and Lawrence's[28] value of 128 emu/g obtained at 77°K in pulsed fields to 140 kOe on a powder specimen provided by G. Fischer of the National Research Council, Ottawa, Canada. We assume α, β, and K to be constants. From x-ray data by Willis and Rooksby[4] one may calculate the density of MnAs at 40°C in the paramagnetic state to be 6.42 g cm^{-3}.

Figure 8 shows plots of Eq. (13) for $H=0$, $P=0$, and T/T_0 ratios of 1.483 to 1.63 for $\alpha\beta T_0=0.25$ and $\eta=3.0$. (These trial values for $\alpha\beta T_0$ and η were chosen after some exploratory analysis.) The net free energy versus magnetization curves are of the same class as curve A of Fig. 2. As was explained in the discussion of that figure, subtraction of the field energy terms $H\sigma_0\sigma/NkT_0$, with the field constants given by the double tangent lines to

[26] See, e.g., C. Kittel, *Introduction to Solid State Physics* (John Wiley & Sons, Inc., New York, 1956), 2nd ed., p. 216.

[27] L. P. Schmid and J. S. Smart, Naval Ordnance Laboratory Report NAVORD 3640, 1954 (unpublished).

[28] D. S. Rodbell and P. E. Lawrence (personal communication).

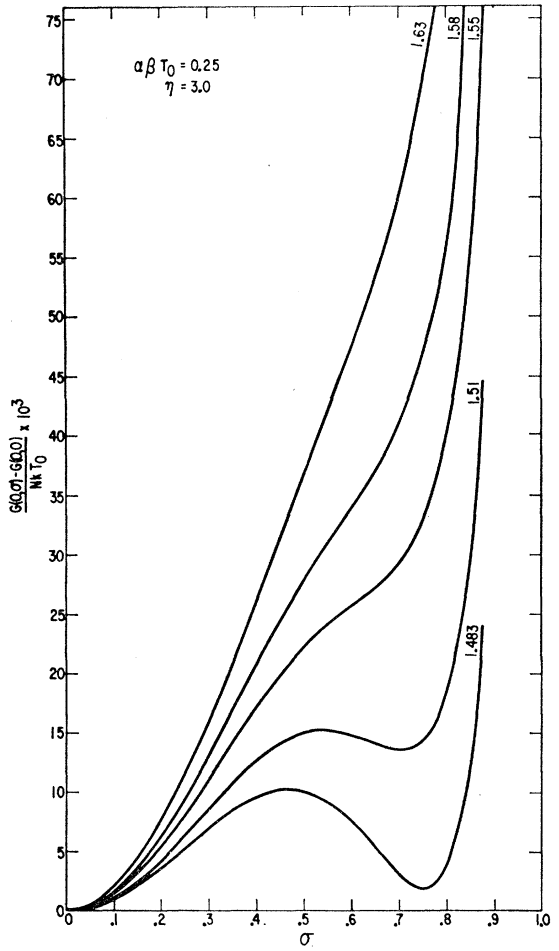

FIG. 8. Free energy vs relative magnetization isotherms at zero field for temperature ratios T/T_0 of 1.483 to 1.63 and for $P=0$, $\alpha\beta T_0=0.25$, and $\eta=3.0$.

the curves of Fig. 8, yields the family of equilibrium curves of Fig. 9 for the given values of T/T_0 and the corresponding listed values of $H\sigma_0/NkT_0$. For example, at $T/T_0=1.55$ and $H\sigma_0/NkT_0=0.04734$ the paramagnetic phase at $\sigma=0.190$ and the ferromagnetic phase at $\sigma=0.695$ are of equal energy and are separated by a potential barrier of height $2.63\times10^{-3}\ NkT_0$ erg g^{-1}. The temperatures and corresponding fields for the curves of Fig. 9 plot into the thermodynamic equilibrium curve B of Fig. 10.

Curve C of Fig. 10 is a plot of field versus temperature, for zero pressure, of the "zero-barrier" condition, corresponding to curve C of Fig. 2. While points on this curve could be obtained by finding the slopes of the curves of Fig. 8 at the first inflection points, it is more accurate to use Eqs. (14) and (15). Substituting a given value of σ in Eq. (15) determines the temperature ratio, T/T_0, for the free energy versus magnetization curve that would have an inflection point at this σ. Substituting these values of T/T_0 and σ in Eq. (14) determines the field that gives zero slope at the inflection point.

We note that the $T/T_0=1.63$ curve of Fig. 9 has no potential barrier and, equivalently, that in Fig. 10 the equilibrium curve B and "zero-barrier" curve C join at this temperature. Thus, the theory predicts a paramagnetic-ferromagnetic critical point that is a function of two of the variables, H, T, and P, for a given set of parameters. Therefore, a first-order transition may only occur if the path a system travels crosses equilibrium curve B below its intersection with curve C.

Curve D of Fig. 10 is a plot of the zero-pressure data of Table I, with the fitted choice of 208.7°K for the value of T_0. This choice brings the experimental data curve D close to "zero-barrier" curve C in the low-field region before the "cliff," and thus implies the assumption of only slight barrier penetration during a pulsed field in this region. A choice of a lower value for T_0 would displace data curve D to the right. (We note here that this value for T_0 is derived with the assumption that α is constant for all temperatures, while actually it must approach zero as T approaches 0°K. Thus, if the temperature variation of α is approximated by having α constant down to about 100°K and zero below that temperature, then the actual T_0 would be higher than the derived value by about 100 $\alpha\beta T_0$ or 25°K.)

The criteria one might hope to see fulfilled in a proper match between theory and data are: (a) The data shall lie within the area between the equilibrium and "zero-barrier" curves B and C. (b) The slope of data curve D at a given temperature shall be close to that of curve C. (If nucleation permits passing through a certain barrier height during a pulsed field, then curve D will be roughly parallel to curve C. If the barrier height pene-

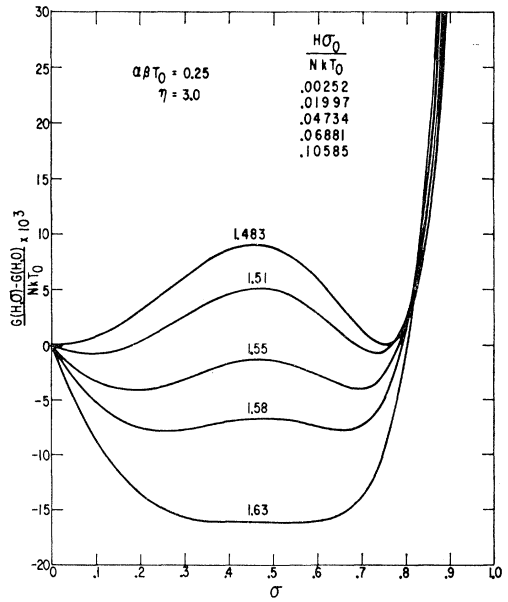

FIG. 9. Free energy vs relative magnetization isotherms of Fig. 8 depressed to paramagnetic-ferromagnetic phase equilibrium conditions by applying the listed magnetic fields.

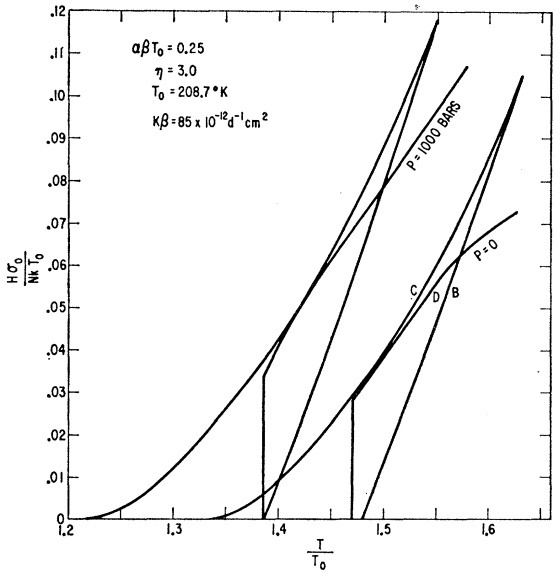

FIG. 10. Magnetic fields vs temperature curves at zero and 1000 bars pressure for paramagnetic-ferromagnetic equilibrium conditions (curve B), for "zero-barrier" condition for transition to the ferromagnetic phase (curve C), and for the experimental data (curve D). The listed values for T_0 and $K\beta$ result from matching the data to the theoretical curves drawn for $\alpha\beta T_0=0.25$ and $\eta=3.0$.

trated becomes larger with increasing field or temperature, then curve D will deviate away from curve C, but never beyond curve B.) (c) The vertical intercept at $H=0$ for the paramagnetic to ferromagnetic transition with decreasing temperature shall be about 5°C below the corresponding intercept of equilibrium curve B. This temperature hysteresis, ΔT, is half the total reported temperature hysteresis of about 10°C.[5] (A 5°C temperature hysteresis would imply the existence in our specimen of an imperfection that is set to transform the specimen as a whole through a potential barrier of about 0.09 J g^{-1} to the energetically favorable ferromagnetic phase at zero applied field and during a time not greater than several minutes. Nevertheless, with the system critically near nucleation to the ferromagnetic phase, a pulse of 29 kOe, which depresses the potential barrier near $\sigma=0.4$ by about 0.15 J g^{-1}, assumedly to near the "zero-barrier" condition of curve C, is required to bring about the transition in a time of several microseconds. Thus, the imperfection, the specific nature of which is unknown, is nearly ineffective in promoting the formation or growth of a nucleus during the microsecond duration of the applied pulsed magnetic field.)

With T_0 chosen as 208.7°K, we next plot the 1000-bar experimental data in Fig. 10. A value of $K\beta$ is then found that gives a "zero-barrier" curve similar to curve C in its relation to the data. The value of $K\beta=85\times10^{-12}$ dyn^{-1}cm^2 thus found is then used to calculate the free energy versus relative magnetization curves of Figs. (11) and (12) for zero and equilibrium values of the field, respectively. The temperatures and corresponding equilibrium fields of Fig. (12) then plot into the 1000-bar equilibrium curve of Fig. 10. (A plot of 500-bar experimental data leads to the same value for $K\beta$ and thus need not be analyzed further.)

Similar analyses for sets of $(\alpha\beta T_0,\eta)$ with values of (0.2,3.0), (0.2,3.5), (0.3,3.0), and (0.3,3.5) yield the field versus temperature curves of Figs. (13) and (14) for pressures of zero and 1000 bars, respectively.

Given the parameters $\alpha\beta T_0$ and η, and the corresponding values of T_0 and $K\beta$ determined by matching theory and experiment, we may use Eq. (7), with $j=\frac{3}{2}$, and Eq. (11) to calculate values for K, β, α, and $T_0{}^*$. Table II lists these various terms and also ΔT, the temperature hysteresis at zero field between the equilibrium curves (e.g., curve B of Fig. 10) and the observed paramagnetic to ferromagnetic transition temperatures for the cooling specimen.

Inspection of the sets of field versus temperature curves with the above imperfectly held criteria in mind indicates that the parameters $(\alpha\beta T_0,\eta)$ lie in the region between (0.20,3.0) and (0.30,3.5), with (0.23,3.2) appearing to be a reasonable compromise. If T_0 and $K\beta$ are now taken, by interpolation, to be 213.4°K and 86×10^{12} dyn^{-1}cm^2, respectively, then β, K, α, and $T_0{}^*$ become 18.9, 4.55×10^{-12} dyn^{-1}cm^2, 5.71×10^{-5}(°C)$^{-1}$, and 277.1°K, respectively. The temperature hysteresis ΔT becomes approximately 5°C.

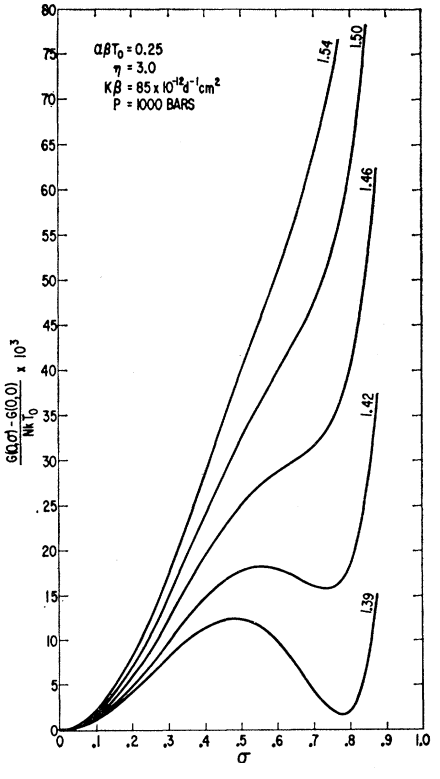

FIG. 11. Free energy vs relative magnetization isotherms at zero field for temperature ratios T/T_0 of 1.39 to 1.54 and for $P=1000$ bars.

TABLE II. Through fit choices of T_0 and $K\beta$ the experimental data of Table I are matched against theoretical curves drawn for the upper five rows of listed values of $\alpha\beta T_0$ and η. This match leads to the corresponding values for the parameters β, K, α, and T_0^*, and for the temperature hysteresis ΔT. The bottom row represents the best match.

$\alpha\beta T_0$	η	$K\beta$ (10^{-12} dyn^{-1} cm^2)	T_0 (°K)	β	K (10^{-12} dyn^{-1} cm^2)	α [10^{-5} (°C)$^{-1}$]	T_0^* (°K)	ΔT (°C) ($P=0$)	ΔT (°C) ($P=1000$ bars)
0.20	3.0	85	223.0	17.2	4.95	5.22	278.8	6.0	4.2
0.20	3.5	87	220.5	19.8	4.39	4.57	275.6	16.8	15.2
0.25	3.0	85	208.7	18.3	4.65	6.56	278.3	2.0	0.2
0.30	3.0		194.5				277.9	−2.3	
0.30	3.5	89	191.8	22.1	4.02	7.07	274.0	6.6	6.2
0.23	3.2	86	213.4	18.9	4.55	5.71	277.1	~5.0	

CHECK ON ANALYTIC RESULTS

Adequate checks for MnAs on the determined values of β, K, and α do not presently exist. Our value for T_0^* of 277.1°K is reasonably close to Serres's[8] experimentally determined value of 285°K, expecially since the transition temperature, and thus probably T_0^*, are sensitive to slight compositional variations.

The value of 18.9 for β, which shows the dependence of Curie temperature T_c on volume, is equivalent here to an increase of 40.3°C per 1% volume strain. A crude check on this value may be made by noting that MnSb, with the same NiAs-type structure as MnAs, has a Curie temperature of 313°C and a cell volume at this temperature that is 1.295 times that of MnAs at 40°C in the paramagnetic phase.[4] The paramagnetic Curie temperature of MnAs is 12°C at this temperature according to Eq. (1). On the crude assumptions that the antimony atoms merely increase the distance through which a given exchange interaction operates and that the stregnth of this interaction increases linearly with volume, we find a Curie temperature increase of 10.2°C per 1% volume strain. The assumption that the Curie temperature varies linearly with nearest neighbor distance, along the c axis, gives a Curie temperature increase of 116°C per 1% c-axis strain.

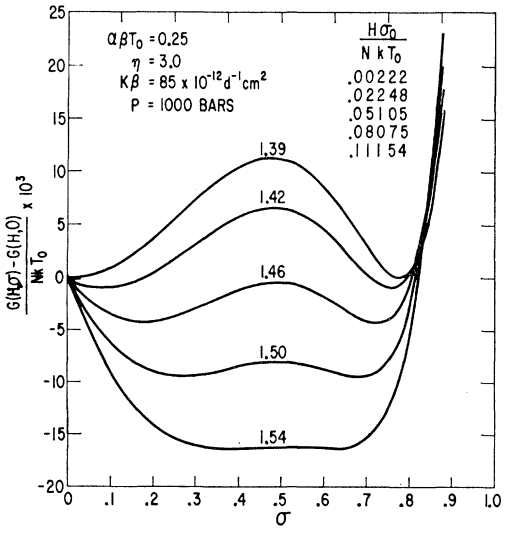

FIG. 12. Free energy vs relative magnetization isotherms of Fig. 11 depressed to paramagnetic-ferromagnetic phase equilibrium conditions by applying the listed magnetic fields.

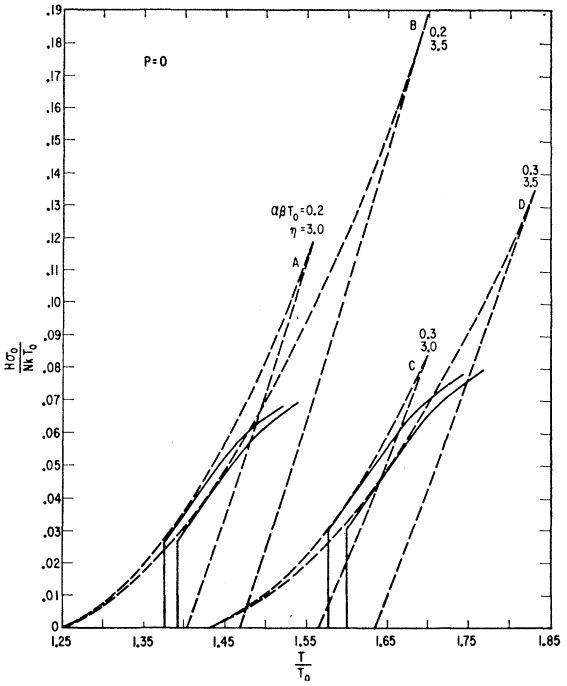

FIG. 13. Magnetic field vs temperature curves similar to those of Fig. 10, but for zero pressure and the noted sets of values for $\alpha\beta T_0$ and η. Note that the four data curves represent the same data for different values of T_0.

The compressibility K has not yet been measured. Our derived value of 4.55×10^{-12} dyn^{-1}cm^2 is double the value recently directly measured[29] for CrTe, a material similar to MnAs in crystal structure. This value thus appears reasonable.

The lattice thermal expansion coefficient α is not directly measurable in the ferromagnetic state. The lattice strain associated with ferromagnetism is larger

[29] N. P. Grazhdankina, L. G. Gaĭdukov, K. P. Rodionov, M. I. Oleĭnik, and V. A. Shchipanov, Zh. Eksperim. i. Teor. Fiz. **40**, 433 (1961) [translation: Soviet Phys.—JETP **13**, 297 (1961)].

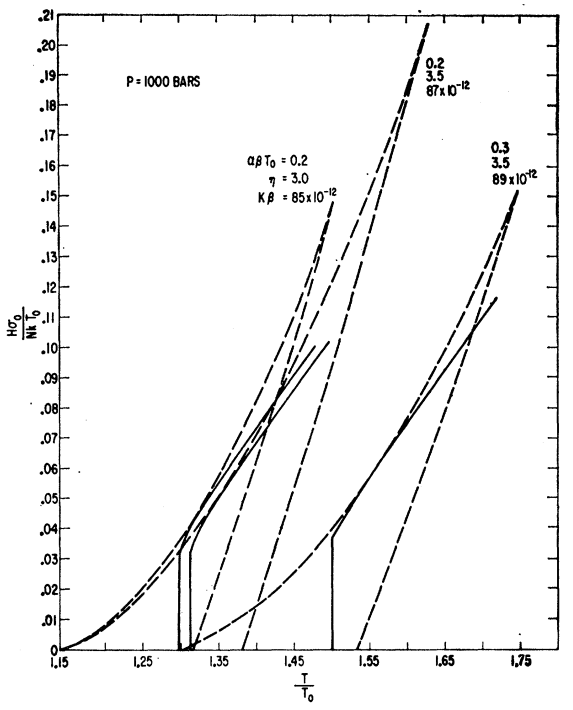

FIG. 14. Magnetic field vs temperature curves similar to those of Fig. 10, but for $P=1000$ bars and the noted sets of values for $\alpha\beta T_0$, η, and $K\beta$.

than the αT term up to the transition, and even leads to a negative net thermal expansion coefficient from O°C to the transition temperature, as is shown by the x-ray studies of Willis and Rooksby[4] and by the more recent ones of Kornelsen.[19] We note further that because of the magnetic lattice strain the value of α is probably not the same as it would be in an unstrained nonmagnetic lattice. The x-ray data of Willis and Rooksby[4] give a volume thermal expansion coefficient of about 24.0×10^{-5}/°C in the paramagnetic phase near 40°C. This is 4.2 times our value for α. By extrapolation to 40°C of the lattice parameter data above the region that we believe is associated with a Jahn-Teller distortion, one obtains a smaller α of about 17×10^{-5}/°C.

The density increase for the ferromagnetic to paramagnetic transition at zero field and pressure is 1.86% according to the x-ray data of Willis and Rooksby.[4] Using the determined values of K, β, and T_0, and a change of relative magnetization from $\sigma_1=0.774$ to $\sigma_2=0$ (from inspection of the available figures of free energy versus relative magnetization), we find that the first term of Eq. (4) gives a density increase of 4.07% for this transition.

Bates[5] and Guillaud's[9] experimentally determined values for the latent heat, $T\Delta S$, for the ferromagnetic to paramagnetic transition at zero field and pressure are 1.79 and 2.4 cal g^{-1}, respectively, where the value 2.4 cal g^{-1} is obtained by our graphical integration of Guillaud's data. Using $\alpha\beta T_0=0.23$, $T=318$°K, and $\sigma_1-\sigma_2=0.774-0$, we find the spin entropy change from the tables of Schmid and Smart,[27] the lattice entropy change from Eqs. (4) and (5), and calculate a net latent heat of 2.48 cal g^{-1}.

Clausius-Clapeyron Equation

The Clausius-Clapeyron equation,

$$dP/dT=L/T\Delta V, \tag{16}$$

relating the slope of a first-order phase transition curve at a given pressure and temperature in a P–T diagram to the reversible latent heat L and volume change ΔV involved in the transition, provides an approximate check among various experimental values. The above experimentally determined latent heats of 1.79 and 2.4 cal g^{-1}, density change of 1.86%, and transition temperature of 318°K at zero pressure and field give slopes of -8.1 and -10.9×10^7 dyn/cm²°C, respectively. The experimental slope in Fig. 6 for the paramagnetic to ferromagnetic transition at zero pressure and field and at 307°K is -4.15×10^7 dyn/cm²°C. Rodbell and Wilson[30] obtain a slope of -8.3×10^7 dyn/cm²°C from measurements of relative magnetization at 12 kOe versus pressure for several temperatures.

We may further use the Clausius-Clapeyron equation in its above form and also in its magnetic form, with H and $\sigma_0\sigma$ replacing P and $-V$, respectively, to check the self-consistency of the theory. Curves such as B of Fig. 10 correspond in the theory to the thermodynamic equilibrium conditions between the ferromagnetic and paramagnetic phases. From Fig. 10 we find the straight line slope, $\Delta P/\Delta T$, at zero field and between the equilibrium curves at zero and 1000 bars to be -5.19 dyn/cm²°C. At zero pressure and for $\sigma_1-\sigma_2=0.755-0$ we calculate the entropy and volume changes as above, finding $\Delta S/\Delta V$ to be -5.14×10^7 dyn/cm²°C. At 1000 bars and for $\sigma_1-\sigma_2=0.780-0$ we calculate $\Delta S/\Delta V$ to be -5.23×10^7 dyn/cm²°C. These two values bracket the straight-line slope and indicate that the theoretical slope at zero field increases in magnitude with increasing pressure.

To check for self-consistency against the magnetic form of the Clausius-Clapeyron equation we first note that the straight-line slope, $\Delta H/\Delta T$, of curve B between $T/T_0=1.51$ and 1.483 is 0.646 $Nk\sigma_0^{-1}$. Then for $\sigma_1-\sigma_2=0.755-0$ we find the spin and lattice entropy changes as above and calculate $-\Delta S/\sigma_0\Delta\sigma$ to be 0.620 $Nk\sigma_0^{-1}$. Since the slope of Curve B increases with increasing field, this slightly smaller zero-field value appears to be an adequate check.

We noted earlier that Meyer and Taglang[25] obtained a change of transition field with temperature of 3.0 kOe/°C in the field of an electromagnet. Since their curves for the two directions of the transition have the

[30] D. S. Rodbell, discussion in *Progress in Very High Pressure Research*, edited, by F. P. Bundy, W. R. Hibbard, Jr., and H. M. Strong (John Wiley & Sons, Inc., New York, 1961), p. 283.

same constant slope, the median thermodynamic-equilibrium curve would probably have the same slope. Using the magnetic form of the Clausius-Clapeyron equation, the determined value of 0.23 for $\alpha\beta T_0$, and a change of relative magnetization $\sigma_1-\sigma_2=0.780-0$, we find $-\Delta S/\sigma_0\Delta\sigma$ to be 0.66 $Nk\sigma_0^{-1}$, or 3.2 kOe/°C.

It is clear from Fig. 10 that pulsed-field data curve D properly has a slope less than that for theoretical equilibrium curve B. Under these nonequilibrium conditions we expect the data to lie more nearly parallel to "zero-barrier" curve C. Between 29 and 50 kOe the slope of curve D is 1.77 kOe/°C. Rodbell and Lawrence [31] obtain a slope of 1.21 kOe/°C using pulsed fields of millisecond duration. The difference between these results is not understood inasmuch as the direction of the difference is opposite to that predicted by the simplest view that the slope would increase with increasing pulse duration.

Adiabatic Heating

In the previous analysis to find α, β, K, and T_0^* we have neglected any temperature rise occurring in the specimen up to the time of the transition. If the spin-lattice relaxation time is sufficiently short, a rising applied field will paramagnetically order the magnetic moments of the spin system, thus decreasing its entropy. In an adiabatic process this change in entropy is transferred to the lattice. The resulting lattice temperature rise may then be found by use of Eqs. (4) and (5) and the entropy tables of Schmid and Smart.[27] If we assume a change of relative magnetization from $\sigma_1=0$ to $\sigma_2=0.25$, a mean temperature of 310°K, and a lattice specific heat of 0.1 cal/g°C,[5] and use the determined value for $\alpha\beta T_0$ of 0.23, we find an adiabatic temperature rise of 2.2°C. For a change to $\sigma_2=0.30$, the adiabatic temperature rise would be 3.0°C. Since Eq. (4) assumes isothermal rather than adiabatic conditions, these results are slightly low, probably by about a percent if the αT term of this equation yields the approximate correction involved.

Since an assumed thermal diffusivity of 0.1 cm^{2}sec^{-1} for MnAs yields a thermal relaxation time for the 25-μ-thick specimen of about 10 μsec, which is also approximately the rise time of the field pulse, the actual temperature rise before the transition will be less than for the adiabatic case. Future experiments showing the change of transition field with change of pulse rise time for a given starting temperature should indicate how close to adiabatic or isothermal the process is. However, even if we assume the process to be adiabatic, the changes in the derived parameters are small. Shifting the zero-pressure temperatures of Table I upward by 2.2°C for 29 kOe to 3.0°C for 70 kOe, matching these data to the field versus temperature curve A of Fig. 13, and assuming $K\beta$ still to be 85×10^{-12} dyn^{-1} cm^2 results in no change in α and changes β from 17.2 to 17.0, K from 4.95 to 4.98×10^{-12} dyn^{-1} cm^2, and T_0 from 223.0 to 224.6°K. There is an accompanying slight decrease in the slope of the data curve. This would increase the chosen value for η by less than 0.1.

The adiabatic temperature rise during the paramagnetic to ferromagnetic transition is calculated as above, but for $\sigma_1=0.25$ and $\sigma_2=0.75$, to be about 21°C. This comparatively large rise indicates that an analysis of hysteresis data for the reverse transition to the paramagnetic phase as the field pulse falls may best await a determination of the temperature at the beginning of this transition.

Magnetocrystalline Anisotropy

Two exploratory experiments show that MnAs has a large uniaxial magnetocrystalline anisotropy with the c axis as the hard direction of magnetization. In the first experiment the 10 μg specimen was under prepulse conditions of 30.4°C and 137 bars, which fall within the region where hysteresis retains the specimen in the ferromagnetic phase as the falling pulse passes through zero field. The beginning of the magnetization reversal is faintly detectable at 15.4 kOe in a photograph of the oscilloscope traces. Neglecting a slight shape anisotropy correction, one may set this anisotropy field equal to $-2K_1/M_s$, where K_1 is the first-order uniaxial anisotropy constant and M_s is the spontaneous magnetization per unit volume. This gives an anisotropy constant of -4.9×10^6 ergs/cm^3 for an M_s of 630 emu/cm^3. For a pulse starting at the same pressure but at a nonequilibrium temperature several degrees higher, the beginning of the reversal was detectable at a lower field of 13.7 kOe.

In the second experiment, to investigate this result further, a 175 μg single-crystal specimen 1.01 mm long (the c axis), 0.34 mm wide, and 0.13 mm thick, from the same batch as the 10-μg specimen, was mounted in a torque magnetometer with the axis of rotation perpendicular to the c axis and to the width. Torque measurements were made at several temperatures in fields of an electromagnet to 23.5 kOe near the zero-torque point of minimum energy (c axis perpendicular to H). A plot of the reciprocal of the slope of the torque curve at this point versus the reciprocal of the magnetic field intercepts the ordinate at $1/(2K^*)$,[32,33] where K^* in our case is the sum of the magnetocrystalline anisotropy, $K_A(=\sum_n nK_n)$, and shape anisotropy K_s. This procedure yields measured anisotropy constants of -1.12, -1.35, -1.62, and -1.77×10^6 ergs/g (or -7.1, -8.5, -10.2, and -11.2×10^6 ergs/cm^3) at 299, 273, 198, and 77°K, respectively. By approximating the specimen shape as a general ellipsoid of the same axial ratios we calculate a correction for shape anisotropy that yields values for K_A of -7.6, -9.0, -11.0, and -12.0×10^6 ergs/cm^3.

[31] D. S. Rodbell and P. E. Lawrence, J. Appl. Phys. **31**, 275S (1960).

[32] J. S. Kouvel and C. D. Graham, Jr., J. Appl. Phys. **28**, 340 (1957).

[33] Henry Shenker, Phys. Rev. **107**, 1246 (1957).

Such a high magnetocrystalline anisotropy leads one to expect that the transition temperature will vary with crystal orientation if the specimen is in a magnetic field. This is apparent since the free energy density for a ferromagnetic specimen of MnAs is less with the basal plane oriented in the field direction than for the c axis oriented along the field. Thus, at a given field the transition temperature to the ferromagnetic phase should be higher for the former orientation. To check this supposition the 175-μg specimen, mounted in the magnetometer, was cooled from the paramagnetic phase in a magnetic field of 18.5 kOe, and the transition temperature to the ferromagnetic phase was observed with the crystal oriented with the c axis (hard direction) parallel to the field and, alternately, nearly perpendicular to the field. The observed transition temperatures differ in the expected direction by about 2.5°C. The transition temperatures with the c axis parallel and perpendicular to the field are 28.1 ± 0.4 and 30.6 ± 0.4°C, respectively. Furthermore, the specimen's transition temperature in zero field is 23.3°C. This is 10.5°C lower than for the 10 μg specimen and probably reflects a compositional variation away from stoichiometric MnAs since its upper transition temperature is only 34°C. Four other grains from the same batch were observed to have lower and upper transition temperatures of (26.0,34.5), (34.2,40), (34.5,39.5), and (34.6,40)°C, respectively.

Recent experiments with another single crystal of MnAs by the authors,[34] to be reported elsewhere, show that a plot of transition temperature versus field for the c axis $\perp H$ is a straight line to the zero-field intercept, and that the plot for the c axis $\|H$ becomes parallel to the c axis $\perp H$ line above the anisotropy field of about 18 kOe. Thus, the temperature difference of 7.3°C (30.6−23.3°C) and corresponding field difference of 18.5 kOe give a slope, $\Delta H/\Delta T$, of 2.5 kOe/°C. As would be expected, this is less than the slope of 3.0 kOe/°C that Meyer and Taglang obtained for a polycrystalline specimen.[31] Use of the Clausius-Clapeyron Eq. (16) in its magnetic form, with $L=1.79$ cal/g,[3] $T=306$°K, and $\sigma_s\Delta\sigma=97$ emu/g,[18] yields a slope of 2.52 kOe/°C.

The isothermal field difference just above 18 kOe, where the curves are found to be parallel, represents a magnetic energy ΔHM_s that equals $\sum_n K_n$, the difference in anisotropy energy for the two orientations. This is clear from the anisotropy energy expression, $E_K=\sum_n K_n \sin^{2n}\theta$, with θ the angle between the magnetization and the c axis of this hexagonal material, and from the shift in the free energy versus σ curves that inclusion of an orientation-dependent energy term must produce for the two orientations. Thus $\sum_n K_n \doteq -2.5$ kOe (°C)$^{-1}\times 2.5$°C$\times 620=-3.9\times10^6$ ergs/cm^3. This result could be combined with the above values for K_A and K_1 to determine approximate values for K_1, K_2, and K_3. The more thorough anisotropy measurements to be reported show that constants K_1, K_2, and K_3, with values of -5.75, $+1.5$, and -1.15×10^6 ergs/cm^3, respectively, are adequate for expressing the anisotropy energy at 35°C.

[34] R. W. DeBlois and D. S. Rodbell, Suppl. J. Appl. Phys. 34, 1101 (1963).

DISCUSSION

The most conspicuous discrepancy between theory and experiment is revealed in the passage of the data curves to the right of the equilibrium curves at higher fields. We noted previously that the data should lie within the regions outlined by the "zero-barrier" and equilibrium curves, such as curves C and B of Fig. 10, if the theory and data are both valid. We consider it probable that this discrepancy is due primarily to a neglect of short-range order in the theory, though part is likely due to the neglect of magnetocrystalline anisotropy and to the assumption that the parameters α, β, and K are constants. As was noted by Bean and Rodbell,[15] the long-range interaction implicit in the molecular-field theory is not in accord with experiment and theory that demonstrate the extreme local character of the exchange interactions that give rise to the ordered state. Since entropy decreases with increasing order and since in the paramagnetic region near the apparent Curie temperature there will be some short-range order even for zero net magnetization, the spin system entropies in this region will be less than those calculated from the tables of Schmid and Smart[27] that consider long-range order only. Furthermore, the specific volumes of the clusters in which short-range order exists will be larger than for the disordered material, as is indicated by the first term of Eq. (4). Thus, the correct specific volume that minimizes the free energy will be somewhat larger than that given by Eq. (4). An attempt to modify the theory to include short-range order is presently being made.

A further clear oversimplification in the theory is the assumption that the exchange energy varies linearly with the lattice specific volume. Ferromagnetic MnAs has a hexagonal NiAs-type crystal structure. The x-ray data of Willis and Rooksby[4] show the nearest-neighbor distance between magnetic atoms just below the transition to be 2.860 Å in the c-axis direction. In the transition, however, it is the next-nearest-neighbor distance, in the basal plane, that changes from 3.715 to 3.681 Å. The c-axis distance remains almost constant. Thus, a more rigorous theory would invoke anisotropic intra-atomic exchange interactions that lead to the observed anisotropic distortions.

We note, finally, that further data of analytic interest remain to be gleaned from the present experiment and from future similar ones. First, we have not yet analyzed the hysteresis data presently available because, as mentioned earlier, the temperature of the specimen as it returns with falling field to the paramagnetic phase is uncertain. Second, the area under the oscilloscope trace of the net pickup-coil voltage is proportional to the change of magnetization at the transition. This change

of magnetization varies within predictable limits with H, T, and P and should, for example, approach zero at critical points that appear readily attainable experimentally. Third, future experiments with an existing MnAs specimen similar to the present one in size and shape, and from the same batch, but with the long axis lying in the basal plane, the direction of easy magnetization, should make clearly visible the area proportional to the spontaneous magnetization of the ferromagnetic specimen as the field passes through zero. Because of the high magnetocrystalline anisotropy, this area, which would be useful to compare against the transition areas, is just barely detectable with the present c-axis oriented specimen and two-turn pickup coil. Fourth, this new specimen should also reveal the effect of magnetocrystalline anisotropy on the transition. It appears from the exploratory experiments of the previous section that the Gibbs free-energy function should include a magnetocrystalline anisotropy term dependent on crystal orientation in the magnetic field and approximately on the third power of the relative magnetization in the region of interest.

CONCLUSION

The moderately good degree of matching between the preceding theoretical and experimental curves, and the reasonable values of the parameters of Table II derived through this match provide a consolidated confirmation of the Bean-Rodbell theory in its cardinal features as applied to MnAs. Added to their previous comparisons of theory and experiments, and to the neutron diffraction work of Bacon and Street[13] and of Kasper and Wilson[17] showing no magnetic order above the 45°C transition, these results validate their deductions that the first-order transition of MnAs from the ferromagnetic phase at 45°C is to the paramagnetic phase and that the transition is energetically a magnetic one arising from a sufficiently sensitive dependence of exchange energy on lattice spacing and a sufficiently large lattice compressibility. Discrepancies between the theory and the experimental results indicate a primary need to include short-range order in a refinement of the theory. Auxiliary experiments show the magnetocrystalline anisotropy of MnAs to be about -7.6 and -12.0×10^6 ergs/cm^3 at 299 and 77°K, respectively.

ACKNOWLEDGMENTS

We are indebted to many of our colleagues for their interest and continuing stimulation. We wish particularly to thank C. P. Bean for many helpful discussions. In addition, we are grateful to V. J. DeCarlo for supplying us with the MnAs specimens and to L. M. Osika for x-ray orientation determination of the 10-μg specimen.